Proceedings of the
44th IEEE Conference on Decision and Control, and
the European Control Conference 2005
Seville, Spain, December 12-15, 2005

Control of a Sphere Rolling on a Plane with Constrained Rolling Motion

Akira Nakashima, Kenji Nagase and Yoshikazu Hayakawa

Abstract— **In this paper, we discuss control of contact coordinates for a contact point between a sphere and a plane with pure rolling contact by using iterative closed paths on the sphere with contstrained rolling motion. We first analyze the boundary of the reachable area by the closed path with constrained rolling motion. Utilizing the result, we second propose a method which converge all the contact coordinates to a target point by the iteration of a finite number of the closed paths. A numerical example where the rolling motion is restricted to the area on the semisphere shows the effectiveness of the proposed method.**

I. INTRODUCTION

In grasp and manipulation of an object by a multi-fingered robot hand, the contact points can be changed *simultaneously* by utilizing rolling contact. Furthermore, due to the nonholonmy of rolling, the system can be driven to any desired configurations using fewer inputs than the degrees of the freedom of the system. For a dynamical model composed of fingers and a grasped object, we proposed a method which could utilize the nonholonomy of rolling for control of contact points simultaneously with grasp and manipulation of the object [1]. In this study, the contact motion is a nonholonmic system of rolling bodies with regular surface. In this paper, for the case where the rolling bodies are a sphere and a plane, we consider the control of the contact coordinates for the contact point.

Since nonholonomic systems of rolling bodies can not be converted to the conventional chained form, the control of the system is somewhat involved. One of the major ideas for controlling the contact coordinates is to utilize the holonomy of specified closed paths. Li *et al.* [3] proposed a path planning of a sphere on a plane by two types of closed paths. Bicchi *et al.* [4] proposed a path planning of a object with a general surface and a plane by two types of closed paths. However, since these studies achieve the regulation of the contact coordinates sequentially by using multiple type of closed paths, a regulation algorithm by using single type of closed path is expected from the viewpoint of robustness against a disturbance. Furthermore, in the case where the above methods are applied to robot hands, it is essential that the constrained rolling motion must be considered since the work spaces of the robot hands are generally limited.

A. Nakashima and Y. Hayakawa are with Dept. of Mechanical Science and Engineering, Graduate School of Engineering, Nagoya University, Furo-cho, Chikusa-ku, Nagoya, 464-8603, Japan {a_nakashima,hayakawa}@nuem.nagoya-u.ac.jp

K. Nagase is with Dept. of Opto-Mechatronics, Faculty of Systems and Engineering, Wakayama University, 930 Sakae-Dani, Wakayama-shi, Wakayama, 640-8510, Japan nagase@sys.wakayama-u.ac.jp

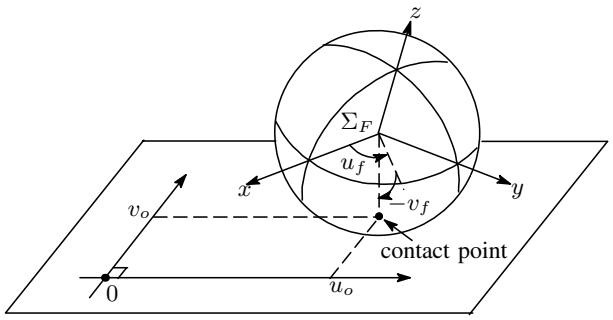

Fig. 1. Spherical finger rolling on a plane.

In this paper, for the kinematic model of a sphere and a plane which correspond to a spherical finger and a cuboid object, we propose a method to regulate all the contact coordinates simultaneously by finite iterative closed paths on the contact point of the sphere. Furthermore, the rolling motion is constrained. The closed path is shaped as a trapezoid on the sphere parameterized by three variables. We call this closed path the *trapezoidal closed path*. Firstly, the reachable area by the closed path is analyzed in detail. Secondly, we propose a method for the contact coordinates to converge to a target point by utilizing the boudaries of the reachable area. Lastly, a numerical example where the rolling motion is restricted to the area on the semisphere shows the effectiveness of the proposed method.

II. CONTROL PROBLEM

In this section, we describe the control problem in which the constrained rolling motion is considered. Figure 1 shows a spherical finger rolling on a plane of a object. The contact points on the sphere and the plane are respectively represented by $\boldsymbol{\alpha}_f \in \mathbb{R}^2$ and $\boldsymbol{\alpha}_o \in \mathbb{R}^2$, which are the spherical coordinates and the orthogonal coordinates. At the contact point, let $\psi \in \mathbb{R}$ be the angle between the directions of u_o and the projection of the latitude (u_f) on the plane. Therefore, the configuration of the system is expressed by the contact coordinates [2]:

$$\boldsymbol{\eta} := [\ \boldsymbol{\alpha}_f^{\mathrm{T}} \quad \boldsymbol{\alpha}_o^{\mathrm{T}} \quad \psi\ ]^{\mathrm{T}} \in \mathbb{R}^5. \tag{1}$$

A type of the rolling contact is assumed to be the pure rolling contact. Then, the kinematic model which represents the relationship between $\dot{\boldsymbol{\eta}}$ and $\dot{\boldsymbol{\alpha}}_f$ is as follows [2]:

$$\begin{bmatrix} \dot{\boldsymbol{\alpha}}_f \\ \dot{\boldsymbol{\alpha}}_o \\ \dot{\psi} \end{bmatrix} = \begin{bmatrix} 1 & 0 \\ 0 & 1 \\ \rho\cos v_f \cos\psi & -\rho\sin\psi \\ -\rho\cos v_f \sin\psi & -\rho\cos\psi \\ \sin v_f & 0 \end{bmatrix} \dot{\boldsymbol{\alpha}}_f, \tag{2}$$

0-7803-9568-9/05/$20.00 ©2005 IEEE

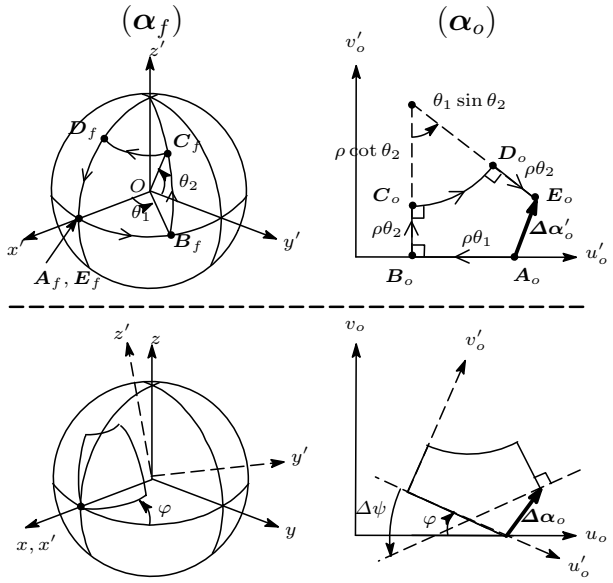

Fig. 2. The trapezoidal closed path on the sphere.

where ρ is the radius of the sphere. For simplicity, a target point is assumed to be the origin of $\boldsymbol{\eta}$ and $\dot{\boldsymbol{\alpha}}_f$ is assumed to be able to controlled directly. Hence, the initial state of $\boldsymbol{\alpha}_f$ is assumed to be the origin. Consequently, the control problem is reduced to be the regulation of

$$\widetilde{\boldsymbol{\eta}} := [\ \boldsymbol{\alpha}_o^{\mathrm{T}} \quad \psi\ ]^{\mathrm{T}} \in \mathbb{R}^3 \tag{3}$$

by iterative closed paths on the sphere.

The closed path on the sphere for the regulation is shown in Fig. 2 (initial condition: $\boldsymbol{\alpha}_f = \mathbf{0}$, $\psi = \pi$). In the upper, the left figure shows the closed path along the path of $\boldsymbol{\alpha}_f$: $A_f \to B_f \to C_f \to D_f \to E_f(A_f)$ which is characterized by the parameters θ_1 and θ_2. Then, the right figure shows the path of $\boldsymbol{\alpha}_f$: $A_o \to B_o \to C_o \to D_o \to E_o$, which is generated by the left closed path. The thick arrow, i.e. $\Delta\boldsymbol{\alpha}'_o$, is the incremental distance of $\boldsymbol{\alpha}_o$ by the left closed path. On the other hand, the lower left figure shows the case where the upper closed path is rotated through the parameter φ about the x'- axis. Then, the lower right figure shows the trajectory of $\boldsymbol{\alpha}_o$ generated by the left closed path, i.e., the path rotated through φ about the normal to the (u_o, v_o) plane. Therefore, the incremental distance of $\boldsymbol{\alpha}_o$ can be obtaned by rotating $\Delta\boldsymbol{\alpha}'_o$ in the upper figure through φ. The incremental distances of $\boldsymbol{\alpha}_o$ and ψ are denoted by $\Delta\boldsymbol{\alpha}_o$ and $\Delta\psi$ respectively. By integrating (2) along the closed path with the initial condition, the incremental distances are given by

$$\Delta\widetilde{\boldsymbol{\eta}} := [\ \Delta\boldsymbol{\alpha}_o^{\mathrm{T}} \quad \Delta\psi\ ]^{\mathrm{T}} \in \mathbb{R}^3, \tag{4}$$

where

$$\Delta\boldsymbol{\alpha}_o(\theta_1, \theta_2, \varphi) = \boldsymbol{R}_\varphi(\varphi)\Delta\boldsymbol{\alpha}'_o(\theta_1, \theta_2) \tag{5}$$

$$\Delta\psi(\theta_1, \theta_2) = -\theta_1 \sin\theta_2 \tag{6}$$

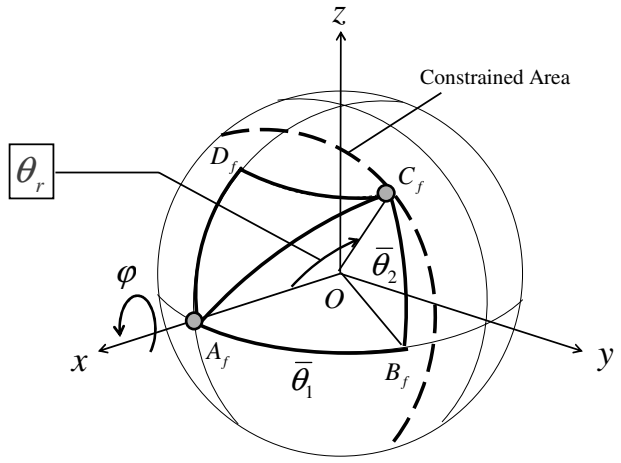

Fig. 3. Constrained area on the surface of the sphere.

$$\boldsymbol{R}_\varphi := \begin{bmatrix} \cos\varphi & \sin\varphi \\ -\sin\varphi & \cos\varphi \end{bmatrix} \tag{7}$$

$$\Delta\boldsymbol{\alpha}'_o = \begin{bmatrix} -\rho\theta_1 + \rho(\cot\theta_2 + \theta_2)\sin(\theta_1\sin\theta_2) \\ \rho(\cot\theta_2 + \theta_2)(1 - \cos(\theta_1\sin\theta_2)) \end{bmatrix}. \tag{8}$$

We call this closed path *trapezoidal closed path*. Note that the closed path is characterized by the parameters $(\theta_1, \theta_2, \varphi)$.

In this paper, the constrained rolling motion is considered. Therefore, the range of θ_1, θ_2 and φ are defined by

$$|\theta_1| \le \bar{\theta}_1, \quad |\theta_2| \le \bar{\theta}_2, \quad |\varphi| \le \pi, \tag{9}$$

where

$$0 < \bar{\theta}_1 < \pi, \quad 0 < \bar{\theta}_2 < \frac{\pi}{2}. \tag{10}$$

Note that the start direction of the closed path, φ, is not constrained. This means that the rolling motion can be generated in arbitrary directions at the start position of the closed path A_f.

Remark 1: In order to apply a method in this paper to control of contact points by multi-fingered robot hands, it is necessary to obtain the area on the sphere by the constrained rolling motion. When the parameters are constrained as in (9) and (10), the constrained area on the sphere is the circled area surrounded by the dashed line shown in Fig. 3. This area is depicted by rotating the point C_f through 2π about x- axis. This circled area is characterized by the angle $\theta_r := \angle A_f O C_f$. It follows that the boundaries of $\boldsymbol{\alpha}_f := [\ u_f \quad v_f\ ]^{\mathrm{T}}$ are

$$|u_f| \le \theta_r, \quad |v_f| \le \theta_r, \tag{11}$$

where

$$\theta_r = \cos^{-1}(\cos\bar{\theta}_1 \cos\bar{\theta}_2) \tag{12}$$

is given by applying Law of cosines to the triangle $\triangle A_f O C_f$.

In the following sections, we propose a method for $\widetilde{\boldsymbol{\eta}}$ to converge to the origin by finite iterative closed paths with constrained rolling motion. The fundamental ideas are composed of the following items:

(1) (Section III) To determine the parameter φ from the viewpoint of the norm minimization independent of the other two parameters. Due to this determination, the control problem can be discussed on the fewer two-dimensional space of $(\|\boldsymbol{\alpha}_o\|, \psi)$ than $\widetilde{\boldsymbol{\eta}} = [\ \boldsymbol{\alpha}_o^{\mathrm{T}} \quad \psi\ ]^{\mathrm{T}} \in \mathbb{R}^3$.
(2) (Section IV) To estimate precisely the boundary of the reachable area by the closed path. The transformation from θ_1 to the other parameter $\varepsilon (= \Delta\psi = -\theta_1 \sin\theta_2)$ is utilized to simplify the analysis.
(3) (Section V) To propose the method for $(\|\boldsymbol{\alpha}_o\|, \psi)$ to converge to the origin by the finite iterative shifts along the boundary. The parameters at each iteration can be easily calculated by the bisection method.

III. Properties of Incremental Distances

In this section, some properties of the incremental distances are shown in order to evaluate the boudary of the reachable area of the closed path.

Firstly, the following fundamental lemma holds.

Lemma 1: $\boldsymbol{\Delta\alpha}'_o$ and $\Delta\psi$ defined by (6) and (8) have the following properties.
(i) $\boldsymbol{\Delta\alpha}'_o$ and $\Delta\psi$ are continuous with respect to (θ_1, θ_2).
(ii) The following equivalent conditions hold:

$$\|\boldsymbol{\Delta\alpha}'_o\| = 0 \Longleftrightarrow \theta_1 = 0 \quad \text{or} \quad \theta_2 = 0, \tag{13}$$

$$\Delta\psi = 0 \Longleftrightarrow \theta_1 = 0 \quad \text{or} \quad \theta_2 = 0. \tag{14}$$

Proof: **(i)** From (6) and (8), it is evident that $\boldsymbol{\Delta\alpha}'_o$ and $\Delta\psi$ are continuous relative to θ_1 and θ_2 except $\theta_2 = 0$, since $\boldsymbol{\Delta\alpha}'_o$ and $\Delta\psi$ are composed of sums and products of $\sin(\cdot)$, $\cos(\cdot)$ and $\cot(\cdot)$. Hence, we investigate the limit value at $\theta_2 \to 0$ of $\boldsymbol{\Delta\alpha}'_o = [\ \Delta u'_o \ \ \Delta v'_o\ ]^{\mathrm{T}}$ because $\Delta u'_o$ and $\Delta v'_o$ include $\cot\theta_2 = \frac{\cos\theta_2}{\sin\theta_2}$. Calculating $\lim_{\theta_2 \to 0} \Delta u'_o$ leads to

$$\lim_{\theta_2 \to 0} \Delta u'_o = -\rho\theta_1 + \lim_{\theta_2 \to 0} \rho \frac{\cos\theta_2 \sin(\theta_1 \sin\theta_2)}{\sin\theta_2}. \tag{15}$$

Applying l'Hospital's theorem to the second term of the right hand side of (15), we get $\lim_{\theta_2 \to 0} = \rho\theta_1$. Therefore, substituting this result into (15) leads to $\lim_{\theta_2 \to 0} \Delta u'_o = 0$. Furthermore, calculating $\lim_{\theta_2 \to 0} \Delta v'_o$ by l'Hospital's theorem similarly, we get $\lim_{\theta_2 \to 0} \Delta v'_o = 0$. Therefore, $\boldsymbol{\Delta\alpha}'_o$ is continuous at $\theta_2 = 0$.

(ii) It is evident from (6) that (14) holds. On the other hand, it is evident from (8) and $\lim_{\theta_2 \to 0} \Delta v'_o = 0$ that the necessity of (13) holds. Next, consider the sufficiency of (13). From (8), the condition equivalent to $\Delta v'_o = 0$ is $\cot\theta_2 + \theta_2 = 0$ or $1 - \cos(\theta_1 \sin\theta_2) = 0$. However, $\cot\theta_2 + \theta_2 \neq 0$ from $-\frac{\pi}{2} < \theta_2 < \frac{\pi}{2}$. Therefore, from $1 - \cos(\theta_1 \sin\theta_2) = 0$, $\Delta v'_o = 0$ holds if and only if $\theta_1 = 0$ or $\theta_2 = 0$ holds. ∎

Secondly, for the parameter φ, i.e. the start direction of the closed path, the following lemma holds.

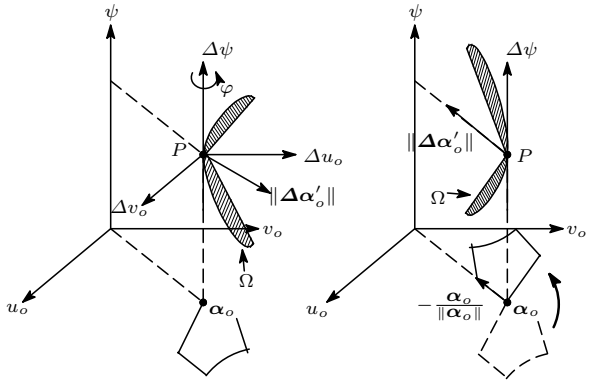

Fig. 4. The interpretation of Lemma 2 form a geometric view point.

Lemma 2: Consider $(\boldsymbol{\Delta\alpha}_o, \Delta\psi)$ defined by (3) and (4). Then, the parameter φ to minimize $\|\widetilde{\boldsymbol{\eta}} + \boldsymbol{\Delta}\widetilde{\boldsymbol{\eta}}\|$ satisfies the following equation:

$$\boldsymbol{R}_\varphi \frac{\boldsymbol{\Delta\alpha}'_o}{\|\boldsymbol{\Delta\alpha}'_o\|} = -\frac{\boldsymbol{\alpha}_o}{\|\boldsymbol{\alpha}_o\|}. \tag{16}$$

Proof: From $\boldsymbol{\Delta}\widetilde{\boldsymbol{\eta}} = [\ (\boldsymbol{R}_\varphi \boldsymbol{\Delta\alpha}'_o)^{\mathrm{T}} \quad \Delta\psi\ ]^{\mathrm{T}}$,

$$\|\widetilde{\boldsymbol{\eta}} + \boldsymbol{\Delta}\widetilde{\boldsymbol{\eta}}\|^2 = \|\boldsymbol{\alpha}_o\|^2 + \psi^2 + \underbrace{2\boldsymbol{\alpha}_o^{\mathrm{T}}(\boldsymbol{R}_\varphi \boldsymbol{\Delta\alpha}'_o)}_{A} + 2\psi\Delta\psi + \|\boldsymbol{\Delta\alpha}'_o\|^2 + \Delta\psi^2,$$

where $\boldsymbol{R}_\varphi^{\mathrm{T}} \boldsymbol{R}_\varphi = \boldsymbol{I}_2$ from (7). In the right side of the above equation, note that terms depending φ are only A and A is the inner product between $\boldsymbol{\alpha}_o$ and $\boldsymbol{R}_\varphi \boldsymbol{\Delta\alpha}'_o$. Therefore, the term A is minimized with respect to φ when the angle made by $\boldsymbol{\alpha}_o$ and $\boldsymbol{R}_\varphi \boldsymbol{\Delta\alpha}'_o$ is π, i.e. φ satisfies (16). ∎

Consider the interpretation of Lemma 2 from a geometric view point. From (4) and (5), the incremental distance $\boldsymbol{\Delta}\widetilde{\boldsymbol{\eta}}$ is rewritten as

$$\boldsymbol{\Delta}\widetilde{\boldsymbol{\eta}} = \begin{bmatrix} \boldsymbol{R}_\varphi \boldsymbol{\Delta\alpha}'_o \\ \Delta\psi \end{bmatrix} = \begin{bmatrix} \|\boldsymbol{\Delta\alpha}'_o\| \left(\boldsymbol{R}_\varphi \dfrac{\boldsymbol{\Delta\alpha}'_o}{\|\boldsymbol{\Delta\alpha}'_o\|} \right) \\ \Delta\psi \end{bmatrix}. \tag{17}$$

This structure of (17) is illustrated in the left hand of Fig. 4. In the left figure, P represents the point of $\widetilde{\boldsymbol{\eta}} = [\ \boldsymbol{\alpha}_o^{\mathrm{T}} \quad \psi\ ]^{\mathrm{T}} = [\ u_o \quad v_o \quad \psi\ ]^{\mathrm{T}}$ in the three-dimensional space of $\widetilde{\boldsymbol{\eta}}$ and the shaded area represents the reachable area of the closed path on the plane $(\|\boldsymbol{\Delta\alpha}'_o\|, \Delta\psi)$ at P with the origin. We call this area Ω. Observing the structure of (17) leads to the fact that the reachable area of $\boldsymbol{\Delta}\widetilde{\boldsymbol{\eta}}$ is obtained by rotating the area Ω through φ about $\Delta\psi$-axis. Therefore, the geometric interpretation of (16) is that φ is determined such that $\|\boldsymbol{\Delta\alpha}'_o\|$- axis coincides $-\frac{\boldsymbol{\alpha}_o}{\|\boldsymbol{\alpha}_o\|}$ as seen in the right figure of Fig. 4. By using φ satisfying (16), the determination problem of $(\theta_1, \theta_2, \varphi)$ for the convergence of $\|\widetilde{\boldsymbol{\eta}} + \boldsymbol{\Delta}\widetilde{\boldsymbol{\eta}}\|$ is reduced to that of (θ_1, θ_2) since $\|\boldsymbol{\Delta\alpha}'_o\|$ and $\Delta\psi$ are functions of θ_1 and θ_2.

Figure 5 shows the concept for $\widetilde{\boldsymbol{\eta}}$ to converge to the target point by using the reachable area Ω. The areas surrounded by dashed lines are the reachable areas Ω at each iteration. As in Fig. 5, $\widetilde{\boldsymbol{\eta}}$ can converges to the target point by shifting

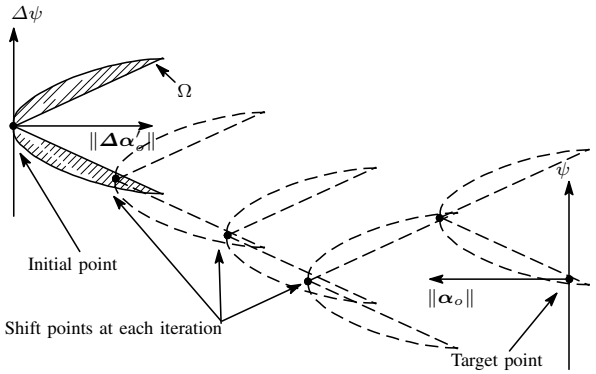

Fig. 5. Concept for $\widetilde{\boldsymbol{\eta}}$ to converge to the target point.

to points on the reachable areas Ω iteratively. To do so, precise analysis of the reachable area Ω is necessary. In the following, the properties of the reachable area Ω at the plane $(\|\Delta\boldsymbol{\alpha}'_o\|, \Delta\psi)$ are investigated.

For the reachable area Ω, the following lemma holds.

Lemma 3: Consider the reachable area Ω at the plane $(\|\Delta\boldsymbol{\alpha}'_o\|, \Delta\psi)$ given by (6) and (8). Then, Ω is symmetry with respect to the $\|\Delta\boldsymbol{\alpha}'_o\|$-axis.

Proof: It is easily checked that $\|\Delta\boldsymbol{\alpha}'_o(\theta_1, \theta_2)\|$ is invariant with respcect to (θ_1, θ_2) such that the sign of $\Delta\psi(\theta_1, \theta_2)$ change. ∎

IV. Evaluation of Boundary of Reachable Area

In this section, we evaluate the boundary of the reachable area of the closed path.

The idea of this section is summarized briefly in Fig. 6. In Fig. 6, the shaded area is the reachable area Ω on the plane $(\|\Delta\boldsymbol{\alpha}'_o\|, \Delta\psi)$, where the part such that $\Delta\psi \geq 0$ of Ω is depicted because the reachable area is symmetry with respect to $\|\Delta\boldsymbol{\alpha}'_o\|$- axis from Lemma 3. The boundary of the reachable area is composed of the boundaries **(A)** and **(B)**, which are represented by the heavy lines **(A)** and **(B)** as in Fig. 6. The line parallel to $\|\Delta\boldsymbol{\alpha}'_o\|$- axis represents the line by $\Delta\psi(\theta_1, \theta_2) = \varepsilon$ and the segment depicted by the heavy line represents the product set of $\Delta\psi(\theta_1, \theta_2) = \varepsilon$ and the reachable area Ω, i.e. $\|\Delta\boldsymbol{\alpha}'_o(-\varepsilon/\sin\theta_2, \theta_2)\|$. Then, the points on the boundary **(A)** corresponds to the points $P_A(\|\Delta\boldsymbol{\alpha}'_o\|, \varepsilon)$ when $\|\Delta\boldsymbol{\alpha}'_o\|$ is minimum and the points on the boundary **(B)** corresponds to the points $P_B(\|\Delta\boldsymbol{\alpha}'_o\|, \varepsilon)$ when $\|\Delta\boldsymbol{\alpha}'_o\|$ is maximum. Therefore, in the following, we investigate the minimum and maximum of $\|\Delta\boldsymbol{\alpha}'_o(-\varepsilon/\sin\theta_2, \theta_2)\|$.

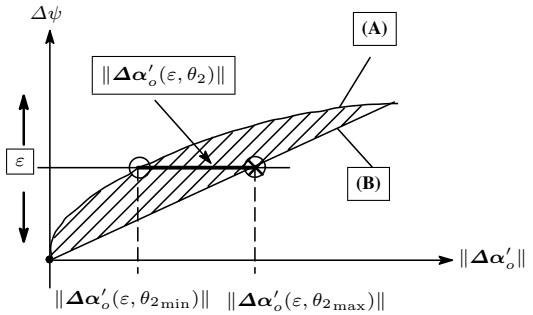

Fig. 6. Reachable area on $(\|\Delta\boldsymbol{\alpha}'_o\|, \Delta\psi)$ plane

For preliminaries of the evaluation, from (6) and (9), the variable θ_1 of $\|\Delta\boldsymbol{\alpha}'_o(\theta_1, \theta_2)\|$ is transformed to ε by the condition

$$\Delta\psi(\theta_1, \theta_2) = -\theta_1 \sin\theta_2 = \varepsilon, \tag{18}$$

where

$$|\varepsilon| \leq \bar{\varepsilon}, \quad \bar{\varepsilon} := \bar{\theta}_1 \sin\bar{\theta}_2. \tag{19}$$

The condition (18) is transformed to

$$\theta_1 = -\frac{\varepsilon}{\sin\theta_2}. \tag{20}$$

Substituting (20) into the domain (9) and solving the resultant inequality with respect to θ_2 lead to the range of θ_2 to guarantee the transformation from θ_1 to ε:

$$-\bar{\theta}_2 \leq \theta_2 \leq \sin^{-1}\left(-\frac{|\varepsilon|}{\bar{\theta}_1}\right) \text{ or } \sin^{-1}\left(\frac{|\varepsilon|}{\bar{\theta}_1}\right) \leq \theta_2 \leq \bar{\theta}_2. \tag{21}$$

By substituting (20) into $\|\Delta\boldsymbol{\alpha}'_o(\theta_1, \theta_2)\|^2$ of (8), $\|\Delta\boldsymbol{\alpha}'_o\|^2$ is transformed to the following function of θ_2 and ε:

$$\|\Delta\boldsymbol{\alpha}'_o(\varepsilon, \theta_2)\|^2 = \rho^2 \frac{\varepsilon^2 - 2\Theta\varepsilon\sin\varepsilon + 2\Theta^2(1-\cos\varepsilon)}{\sin^2\theta_2}, \tag{22}$$

where

$$\Theta(\theta_2) := \cos\theta_2 + \theta_2 \sin\theta_2. \tag{23}$$

Note that $\|\Delta\boldsymbol{\alpha}'_o(-\frac{\varepsilon}{\sin\theta_2}, \theta_2)\|$ $(= \|\Delta\boldsymbol{\alpha}'_o(\theta_1, \theta_2)\|)$ is rewritten as $\|\Delta\boldsymbol{\alpha}'_o(\varepsilon, \theta_2)\|$ for simple description. The function (22) is continuous with respect to ε and θ_2 since ε $(= -\theta_1 \sin\theta_2)$ and $\Delta\boldsymbol{\alpha}'_o(\theta_1, \theta_2)$ are continuous with respect to θ_1 and θ_2 from Lemma 1 (i). Since $\|\Delta\boldsymbol{\alpha}'_o\|$ is symmetry with respect to the ε $(=\Delta\psi)$- axis from Lemma 3 and $\|\Delta\boldsymbol{\alpha}'_o(\varepsilon, \theta_2)\| = \|\Delta\boldsymbol{\alpha}'_o(\varepsilon, -\theta_2)\|$ holds from (22), the case such that $\varepsilon > 0$ and $\theta_2 > 0$ is only considered in the following.

Consider investigating the property of $\|\Delta\boldsymbol{\alpha}'_o(\varepsilon, \theta_2)\|$ with respect to θ_2 in the ranges $0 < \theta_2 < \frac{\pi}{2}$ and $0 < \varepsilon < \pi$ from (9) and (19). Then the following theorem holds.

Theorem 1: Suppose that $\|\Delta\boldsymbol{\alpha}'_o(\varepsilon, \theta_2)\|^2$ is the function of θ_2, ε is the parameter of the function and the ranges of θ_2 and ε are $0 < \theta_2 < \frac{\pi}{2}$, $0 < \varepsilon < \pi$. Then, the following properties hold.

(i) $\varepsilon < \frac{\pi}{2}$: The function has only one minimum value with respect to θ_2.
(ii) $\varepsilon \geq \frac{\pi}{2}$: The function is a monotone decreasing function with respect to θ_2.

Proof: Partial differentiation of (22) with respect to θ_2 is given by

$$\frac{\partial}{\partial\theta_2}\|\Delta\boldsymbol{\alpha}'_o(\varepsilon, \theta_2)\|^2 = \frac{2\rho^2\cos\theta_2}{\sin^3\theta_2} f(\varepsilon, \theta_2), \tag{24}$$

where

$$f(\varepsilon,\theta_2) := \varepsilon\sin\varepsilon\Theta_1(\theta_2) - 2(1-\cos\varepsilon)\Theta_2(\theta_2) - \varepsilon^2, \quad (25)$$

$$\begin{cases} \Theta_1(\theta_2) := 2\cos\theta_2 + \theta_2\sin\theta_2 \\ \Theta_2(\theta_2) := \cos\theta_2(\cos\theta_2 + \theta_2\sin\theta_2) \end{cases}. \quad (26)$$

Since $\cos\theta_2/\sin^3\theta_2 > 0$ from $\theta_2 > 0$, the sign of (24) is determined by $f(\varepsilon,\theta_2)$. In order to analyze (25), Eq. (25) is transformed to

$$f(\varepsilon,\theta_2) = \varepsilon^2\left[\frac{\sin\varepsilon}{\varepsilon}\left\{\Theta_1 - \left(\frac{\tan\frac{\varepsilon}{2}}{\frac{\varepsilon}{2}}\right)\Theta_2\right\} - 1\right], \quad (27)$$

where the following transformation given by the formulas for the double and half angle is utilized:

$$2\frac{1-\cos\varepsilon}{\varepsilon\sin\varepsilon} = 2\frac{2\sin^2\frac{\varepsilon}{2}}{\varepsilon\times 2\sin\frac{\varepsilon}{2}\cos\frac{\varepsilon}{2}} = \frac{\tan\frac{\varepsilon}{2}}{\frac{\varepsilon}{2}}.$$

Partial differentiation of (27) with respect to θ_2 is given by

$$\frac{\partial}{\partial\theta_2}f(\varepsilon,\theta_2) = \varepsilon\sin\varepsilon\Theta_1'\left\{1 - \left(\frac{\tan\frac{\varepsilon}{2}}{\frac{\varepsilon}{2}}\right)\frac{\Theta_2'}{\Theta_1'}\right\}. \quad (28)$$

In order to investigate the sign of (28), the terms in the right hands of (28) and (27) are investigated in the following.

(i) $\frac{\sin\varepsilon}{\varepsilon}$: The differential of $\frac{\sin\varepsilon}{\varepsilon}$ is given by $(\varepsilon\cos\varepsilon - \sin\varepsilon)/\varepsilon^2 < 0$ ($\frac{\pi}{2} \le \varepsilon < \pi$). Let consider the case $0 < \varepsilon < \frac{\pi}{2}$. Since the differentials of ε and $\tan\varepsilon$ at $\theta_2 = 0, \frac{\pi}{2}$ are $\varepsilon'\big|_{\varepsilon=0,\frac{\pi}{2}} = 1$, $\lim_{\varepsilon\downarrow 0}(\tan\varepsilon)' = 1$ and $\lim_{\varepsilon\uparrow\frac{\pi}{2}}(\tan\varepsilon)' = \infty$, the following inequality is holds:

$$\left(\frac{\sin\varepsilon}{\varepsilon}\right)' = \frac{\varepsilon\cos\varepsilon - \sin\varepsilon}{\varepsilon^2} = \frac{\cos\varepsilon}{\varepsilon^2}(\varepsilon - \tan\varepsilon) < 0.$$

Therefore, $\frac{\sin\varepsilon}{\varepsilon}$ is a monotone decreasing function. From $\lim_{\varepsilon\downarrow 0}\frac{\sin\varepsilon}{\varepsilon} = 1$, it follows that the following equation holds:

$$0 < \frac{\sin\varepsilon}{\varepsilon} < 1. \quad (29)$$

(ii) $\frac{\tan\frac{\varepsilon}{2}}{\frac{\varepsilon}{2}}$: From (29), since the differential of $\frac{\tan\frac{\varepsilon}{2}}{\frac{\varepsilon}{2}}$ is given by

$$\left(\frac{\tan\frac{\varepsilon}{2}}{\frac{\varepsilon}{2}}\right)' = \frac{\varepsilon - 2\sin\frac{\varepsilon}{2}\cos\frac{\varepsilon}{2}}{\varepsilon^2\cos^2\frac{\varepsilon}{2}} = \frac{1-\frac{\sin\varepsilon}{\varepsilon}}{\varepsilon\cos^2\frac{\varepsilon}{2}} > 0,$$

$\frac{\tan\frac{\varepsilon}{2}}{\frac{\varepsilon}{2}}$ is a monotone increasing function. By using l'Hospital's theorem, we get $\lim_{\varepsilon\downarrow 0}\frac{\tan\frac{\varepsilon}{2}}{\frac{\varepsilon}{2}} = 1$. Therefore, the following equation holds:

$$\frac{\tan\frac{\varepsilon}{2}}{\frac{\varepsilon}{2}} > 1. \quad (30)$$

(iii) Θ_1', Θ_2': From (26), the differentials of Θ_1 and Θ_2 are given by

$$\Theta_1' = \theta_2\cos\theta_2 - \sin\theta_2, \quad (31)$$

$$\Theta_2' = \tfrac{1}{2}(2\theta_2\cos 2\theta_2 - \sin 2\theta_2). \quad (32)$$

By introducing the following equation

$$g(x) := x\cos x - \sin x, \quad 0 < x < \pi, \quad (33)$$

Eqs. (31) and (32) are represented by

$$\Theta_1' = g(\theta_2), \quad \Theta_2' = \tfrac{1}{2}g(2\theta_2). \quad (34)$$

Since the properties of $g(x)$ are

$$g'(x) = -x\sin x < 0, \quad \lim_{x\downarrow 0} g(x) = 0, \quad (35)$$

the inequality $g(x) < 0$ holds. Therefore, the following inequalities hold:

$$\Theta_1' < 0, \quad \Theta_2' < 0. \quad (36)$$

(iv) $\frac{\Theta_2'}{\Theta_1'}$: From (34), (35), the differential of $\frac{\Theta_2'}{\Theta_1'}$ is given by

$$\left(\frac{\Theta_2'}{\Theta_1'}\right)' = \frac{\theta_2\sin\theta_2}{2\{g(\theta_2)\}^2}h(\theta_2), \quad (37)$$

where

$$h(\theta_2) := -8\cos\theta_2 g(\theta_2) + g(2\theta_2). \quad (38)$$

From (35), the differential of $h(\theta_2)$ is given by $h'(\theta_2) = 8\sin\theta_2 g(\theta_2) < 0$. Therefore, since $\lim_{\theta_2\downarrow 0} h(\theta_2) = 0$ from (38), the inequality $h(\theta_2) < 0$ holds. From (37), since the differential $\left(\frac{\Theta_2'}{\Theta_1'}\right)'$ is negative, the term $\frac{\Theta_2'}{\Theta_1'}$ is a monotone decreasing function. Therefore, from (33) and (34), since the infimum of $\frac{\Theta_2'}{\Theta_1'}$ is given by $\lim_{\theta_2\uparrow\frac{\pi}{2}}\frac{\Theta_2'}{\Theta_1'} = \frac{\pi}{2}$, the following equation holds:

$$\frac{\Theta_2'}{\Theta_1'} > \frac{\pi}{2}. \quad (39)$$

From the analyses **(i)**–**(iv)**, the following inequality holds:

$$\frac{\partial f}{\partial\theta_2} = \underbrace{\varepsilon\sin\varepsilon}_{>0}\underbrace{\Theta_1'}_{<0}\left\{1 - \underbrace{\left(\frac{\tan\frac{\varepsilon}{2}}{\frac{\varepsilon}{2}}\right)}_{>1}\underbrace{\frac{\Theta_2'}{\Theta_1'}}_{>\frac{\pi}{2}}\right\} > 0. \quad (40)$$

Therefore, $f(\varepsilon,\theta_2)$ of (27) is a monotone increasing function of θ_2 irrespective of ε.

Next, from (27), (26), (29) and (30), the limit values of $f(\varepsilon,\theta_2)$ with respect to $\theta_2 \to 0$ and $\theta_2 \to \frac{\pi}{2}$ are given by

$$\lim_{\theta_2\downarrow 0} f(\varepsilon,\theta_2) = \varepsilon^2\left[\frac{\sin\varepsilon}{\varepsilon}\left\{2 - \left(\frac{\tan\frac{\varepsilon}{2}}{\frac{\varepsilon}{2}}\right)\right\} - 1\right] < 0, \quad (41)$$

$$\lim_{\theta_2\uparrow\frac{\pi}{2}} f(\varepsilon,\theta_2) = \varepsilon^2\left[\frac{\pi}{2}\left(\frac{\sin\varepsilon}{\varepsilon}\right) - 1\right]\begin{cases} > 0 & (0 < \varepsilon < \frac{\pi}{2}) \\ \le 0 & (\frac{\pi}{2} \le \varepsilon < \pi) \end{cases} \quad (42)$$

First, consider the case $0 < \varepsilon < \frac{\pi}{2}$. From (41) and (42), there exists θ_2 in the neighborhood of $\theta_2 = 0$ such that the value of $f(\varepsilon,\theta_2)$ is negative and there exists θ_2 in the neighborhood of $\theta_2 = \frac{\pi}{2}$ such that $f(\varepsilon,\theta_2)$ is positive. Therefore, since $f(\varepsilon,\theta_2)$ is a monotone increasing function, the equation $f(\varepsilon,\theta_2) = 0$ has only a solution. Define the solution of $f(\varepsilon,\theta_2) = 0$ by θ_2^*. From (24), $\|\Delta\boldsymbol{\alpha}_o'(\varepsilon,\theta_2)\|^2$ has a minimum value at $\theta_2 = \theta_2^*$. This proves the claim **(i)**. Second, consider the case $\frac{\pi}{2} \le \varepsilon < \pi$. From (41) and (42), the function $f(\varepsilon,\theta_2)$ is always negative. Therefore, from (24), the function $\|\Delta\boldsymbol{\alpha}_o'(\varepsilon,\theta_2)\|^2$ is a monotone decreasing function. This proves the claim **(ii)**. ∎

Figure 7 shows the shapes of the function $\|\Delta\boldsymbol{\alpha}_o'(\varepsilon,\theta_2)\|$ described in Theorem 1. The case $\varepsilon < \frac{\pi}{2}$ is depicted in the left figure, where the value of $\|\Delta\boldsymbol{\alpha}_o'(\varepsilon,\theta_2)\|$ takes a minimal value at $\theta_2 = \theta_2^*$. On the other hand, the case $\varepsilon \le \frac{\pi}{2}$ is depicted in the right figure, where $\|\Delta\boldsymbol{\alpha}_o'(\varepsilon,\theta_2)\|$ is a monotone decreasing function.

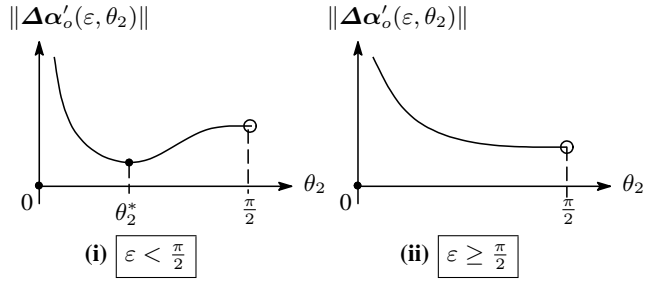

Fig. 7. Sckech of $\|\Delta\boldsymbol{\alpha}'_o(\varepsilon,\theta_2)\|$ as a function of θ_2

Since the property of $\|\Delta\boldsymbol{\alpha}'_o(\varepsilon,\theta_2)\|$ is evident from Theorem 1, it is possible to estimate the boundaries of the reachable area Ω. To be more precise, for each ε in the range (19), it is possible to obtain the values of θ_2 to give the minimum and maximum values of $\|\Delta\boldsymbol{\alpha}'_o(\varepsilon,\theta_2)\|$ in the domain of θ_2 (21) (See Fig. 6). For simplicity, the coordinates $\|\Delta\boldsymbol{\alpha}'_o\|$ and $\Delta\psi$ are represented by

$$x := \|\Delta\boldsymbol{\alpha}'_o(\varepsilon,\theta_2)\|, \quad y := \varepsilon \tag{43}$$

and the values of x on the boudaries (A) and (B) are defined by

$$x_A(\varepsilon) := \|\Delta\boldsymbol{\alpha}'_o(\varepsilon,\theta_{2\min})\|, \; x_B(\varepsilon) := \|\Delta\boldsymbol{\alpha}'_o(\varepsilon,\theta_{2\max})\|, \tag{44}$$

where $\theta_{2\min}$ and $\theta_{2\max}$ gives the minimum and maximum values of x. Condider the case (i). In the case where θ_2^* is included in the domain (21), $\theta_{2\min} = \theta_2^*$ and $\theta_{2\max}$ is given by the supremum or the infimum of (21). In the case where θ_2^* is not included in the domain, if $\bar{\theta}_2 < \theta_2^*$, $\theta_{2\min} = \bar{\theta}_2$ and $\theta_{2\max} = \sin^{-1}\left(\frac{\varepsilon}{\bar{\theta}_1}\right)$. If $\theta_2^* < \sin^{-1}\left(\frac{\varepsilon}{\bar{\theta}_1}\right)$, $\theta_{2\min} = \sin^{-1}\left(\frac{\varepsilon}{\bar{\theta}_1}\right)$ and $\theta_{2\max} = \bar{\theta}_2$. Next, in the case (ii), it is evident that $\theta_{2\min} = \bar{\theta}_2$ and $\theta_{2\max} = \sin^{-1}\left(\frac{\varepsilon}{\bar{\theta}_1}\right)$.

Remark 2: In the case **(i)**, since θ_2^* is the solution of $f(\varepsilon,\theta_2) = 0$ as mentioned in the proof of Theorem 1, it is necessary to obtain the solution by a numerical calculation. This value can be easily calculated by the bisection method since $f(\varepsilon,\theta_2)$ is a monotone increasing function in the range $[0, \frac{\pi}{2}]$ and the signs of $f(\varepsilon,\theta_2)$ are different each other at $\theta_2 = 0, \frac{\pi}{2}$ from (41) and (42).

V. Algorithm for Determination of Parameters

In this section, we propose a method for $(\|\boldsymbol{\alpha}_o\|,\psi)$ to converge to the origin (target point) by the finite iterative shifts along the boundaries on the reachable area Ω on $(\|\Delta\boldsymbol{\alpha}'_o\|,\Delta\psi)$. In the following, the plane $(\|\Delta\boldsymbol{\alpha}'_o\|,\Delta\psi)$ is called the plane (x,y).

First, the reachable area by two iteration of the closed path is characterized as in Fig. 8. The negative range of $x(\|\Delta\boldsymbol{\alpha}'_o\|)$- axis is depicted for explanation. This negative range can be given by transforming φ of (16) into $\varphi + \pi$. The shaded areas represent the reachable areas by one iteration. Furthermore, The area surrounded by the heavy line represents the reachable area by two iteration, which is obtained by depicting Ω at points on the boundaries of

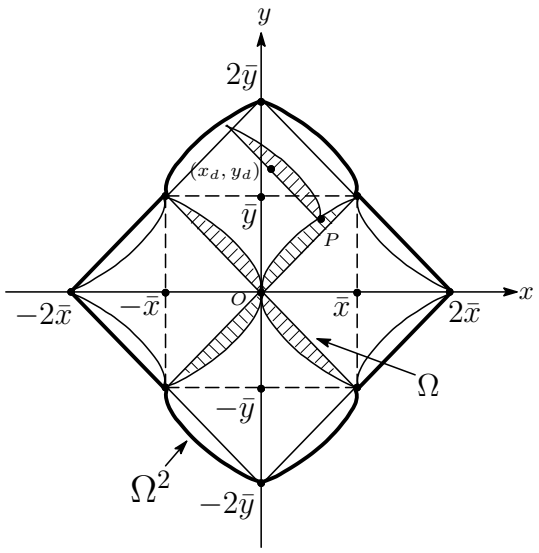

Fig. 8. Reachable area by the iteration of two closed paths

Ω. We call this area Ω^2. The origin O represents the initial point of $(\|\boldsymbol{\alpha}_o\|,\psi)$ and the point (x_d, y_d) is the target point. Then, since the reachable area Ω with the origin P includes the target point (x_d, y_d), it is realized by two iteration for $(\|\boldsymbol{\alpha}_o\|,\psi)$ to converge to (x_d, y_d). The two iteration is composed of the first shift toward P and the second shift toward (x_d, y_d) along the bound (B). The values $\bar{x}$ and $\bar{y}$ represent the coordinate of the end point of Ω and they are the maximum values of x and y respectively. Thus, from (44), $\bar{x}$ and $\bar{y}$ are defined by

$$\bar{x} := x_A(\bar{\varepsilon}) = x_B(\bar{\varepsilon}), \quad \bar{y} := \bar{\varepsilon}. \tag{45}$$

Second, for the determination of the parameters, the plane (x,y) of Fig. 8 is decomposed by the heavy lines as shown in Fig. 9. As mentioned previously, note that there exists the target point in the first or fourth quadrant since the parameter φ is determined by (16). Furthermore, since the reachable area Ω^2 is symmetry with respect to x- axis, we

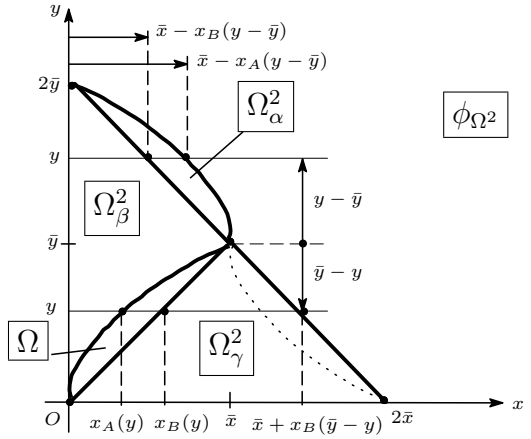

Fig. 9. Decomposition of (x,y) plane

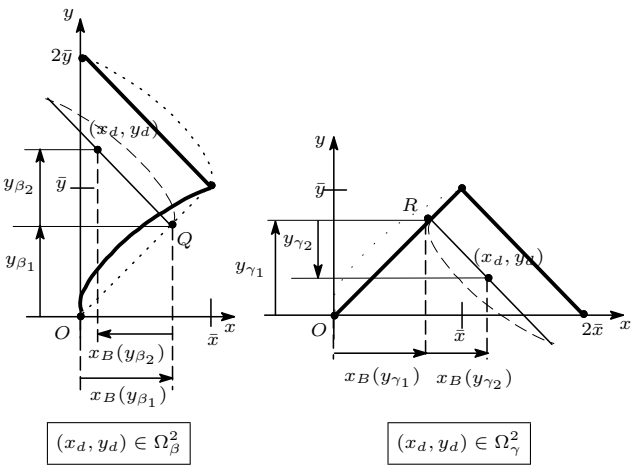

Fig. 10. Scheme of the algorithm for decision of parameters

consider the case the target point exists in the first quadrant. These are the reason why the first quadrant is only shown in Fig. 9. Figure 9 shows that the first quadrant is decomposed into the five areas Ω, Ω^2_α, Ω^2_β, Ω^2_γ and ϕ_{Ω^2}. These areas are defined by

$$\begin{aligned}
\Omega &:= \{(x,y) \,|\, x_A(y) \le x \le x_B(y),\ y \le \bar{y}\},\\
\Omega^2_\alpha &:= \{(x,y) \,|\, \bar{x} - x_B(y-\bar{y}) \le x \le \bar{x} - x_A(y-\bar{y}),\\
&\qquad\qquad \bar{y} < y \le 2\bar{y}\},\\
\Omega^2_\beta &:= \{(x,y) \,|\, x < x_A(y),\ y \le \bar{y} \ \text{ or }\\
&\qquad\qquad x < \bar{x} - x_B(y-\bar{y}),\ \bar{y} < y < 2\bar{y}\},\\
\Omega^2_\gamma &:= \{(x,y) \,|\, x_B(y) < x \le \bar{x} + x_B(\bar{y}-y),\ y < \bar{y}\},\\
\phi_{\Omega^2} &:= \{(x,y) \,|\, x, y \notin \Omega^2,\ \Omega^2 = \Omega \cup \Omega^2_\alpha \cup \Omega^2_\beta \cup \Omega^2_\gamma\},
\end{aligned} \tag{46}$$

where Ω is the reachable area by one iteration, Ω^2_α, Ω^2_β and Ω^2_γ are the reachable area by two iteration and ϕ_{Ω^2} is the area by the more iteration.

Third, in the cases that the target point exists in the above decomposed areas, the method of the shift along the boundaries **(A)** and **(B)** is proposed. The origin O is the initial point and the point (x_d, y_d) represents the target point. The fundamental concept of the proposed method is composed of the followings:

(1) In the case where (x_d, y_d) is included in ϕ_{Ω^2}, to iterate the shift to the end point $(\bar{x}, \bar{y})$ of the reachable area Ω at each iteration until the target point is involved in Ω^2. Since the distances of the shifts have finite values, the target point can be involved in the reachable area Ω^2 by finite iteration.

(2) In the case that (x_d, y_d) is included in Ω^2, to determine the first shift of the two iteration as following ways for the target point to be involved in Ω:

(2)-(i) The target point is involved in Ω^2_α:
(x_d, y_d) is involved in the reachable area Ω by the shift to the end point $(\bar{x}, \bar{y})$ of Ω^2 (See Fig. 9).

(2)-(ii) The target point is involved in Ω^2_β or Ω^2_γ:
The details of the determination are shown later.

(3) In the case that there exists the target point (x_d, y_d) in the reachable area $\Omega \subset \Omega^2$, to shift to the target point by solving the following equation:

$$x(y_d, \theta_2) - x_d = 0, \quad \begin{cases} \theta_{2\min} \le \theta_2 \le \theta_{2\max} \\ \theta_{2\max} \le \theta_2 \le \theta_{2\min} \end{cases} \text{ or } \quad . \tag{47}$$

The details of **(2)-(ii)** is shown in the followings:

(2)-(ii) The target point is involved in Ω^2_β:

In this case as in the left hand of Fig. 10, to shift to the point Q along the boundary **(B)** of Ω at first iteration. Note that Q is the point such that the target point (x_d, y_d) is involved in the boundary **(B)** of Ω depicted at Q. Let define the first and second distances of the shifts of y direction by $y_{\beta_1} > 0$ and $y_{\beta_2} > 0$ respectively. Then, the distances of the shifts of x direction by each iteration are given by $x_B(y_{\beta_1})$ and $x_B(y_{\beta_2})$ from (44). Therefore, the condition such that the point Q must satisfy is as follows:

$$\begin{cases} x_B(y_{\beta_1}) - x_B(y_{\beta_2}) &= x_d \\ y_{\beta_1} + y_{\beta_2} &= y_d \end{cases} . \tag{48}$$

Combining two equations of (48) leads to

$$x_B(y_{\beta_1}) - x_B(y_d - y_{\beta_1}) = x_d, \tag{49}$$

where the range of y_{β_1} is $0 < y_{\beta_1} < y_d$ in the case $y_d < \bar{y}$ or $0 < y_{\beta_1} < \bar{y}$ in the case $y_d \ge \bar{y}$ since $y_{\beta_1} < y_d$ from $y_{\beta_2} = y_d - y_{\beta_1} > 0$ and $y_{\beta_1} < \bar{y}$. Since (49) is a only one variable nonlinear function about y_{β_1} and can be easily solved on this range as mentinoned in Remark 3 later, we can get the coordinate of Q from (44) and (47). By shifting to Q, the target point is involved in Ω at second iteration.

(2)-(ii) The target point is involved in Ω^2_γ:

In this case as in the right hand of Fig. 10, to shift to the point R along the boundary **(B)** of Ω at first iteration. The first and second distances of the shifts of y direction are defined by $y_{\gamma_1} > 0$ and $y_{\gamma_2} < 0$ respectively. By the similar way, we get the following equation:

$$x_B(y_{\gamma_1}) + x_B(y_d - y_{\gamma_1}) = x_d, \tag{50}$$

where the range of y_{γ_1} is $y_d < y_{\gamma_1} \le \bar{y}$ since $y_d < y_{\gamma_1}$ from $y_{\gamma_2} = y_d - y_{\gamma_1} < 0$ and $y_{\gamma_1} \le \bar{y}$. Therefore, the coordinate of R is obtained. By shifting to the obtained point R, the target point is involved in Ω at second iteration.

Remark 3: In the above algorithm, it is necessary to solve (49), (50) and (47) by a numerical calculation. However, the left functions of these equations are one value nonlinear equation with the fixed domains and the signs of the functions at the left and right ends of the domains are different each other. This fact easily follows from the definitions (46) of the areas Ω, Ω^2_β and Ω^2_γ. Therefore, these equations can be easily solved by the bisection method.

Remark 4: Since the parameters $(\theta_1, \theta_2, \varphi)$ can be obtained only from $\widetilde{\boldsymbol{\eta}}$, the method can be interpreted as a discrete-time feedback by regarding the start time of the iteration as the sampling instant. Therefore, the method is expected to have robustness against disturbances.

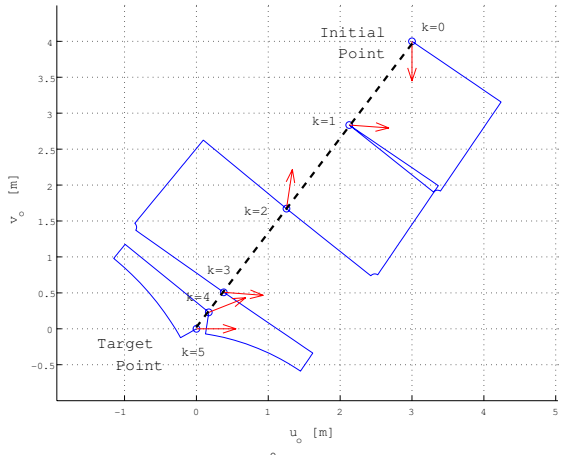

Fig. 11. Trajectory of $\boldsymbol{\alpha}_o$ and ψ on $\boldsymbol{\alpha}_o$ plane

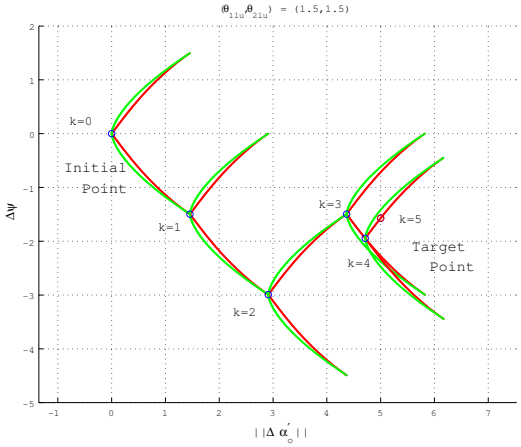

Fig. 12. Shift of $(\|\boldsymbol{\alpha}_o\|, \psi)$ on $(\|\boldsymbol{\Delta\alpha}'_o\|, \Delta\psi)$ plane

VI. Numerical Example

In this section, the effectiveness of the algorithm proposed in the previous section is shown by a numerical example. The radius of the sphere is $\rho = 1$[m]. The initial states are $\boldsymbol{\alpha}_f = [\ 0 \quad 0\ ]^{\mathrm{T}}$[rad], $\boldsymbol{\alpha}_o = [\ 3 \quad 4\ ]^{\mathrm{T}}$[m] and $\psi = \frac{\pi}{2}$[rad]. Furthermore, the value of the boundary of the rolling motion θ_r is set to $\theta_r \approx 1.56 < \frac{\pi}{2}$, which means the case that the contact point on the sphere $\boldsymbol{\alpha}_f = [\ u_f \quad v_f\ ]^T$ is restricted to the area on the semisphere. This value is given by (12) with $\bar{\theta}_1 = \bar{\theta}_2 = 1.5 < \frac{\pi}{2}$.

Figures 11–13 show the simulation result. k is the number of the iteration. Figure 11 shows the shifts of $\boldsymbol{\alpha}_o$ on the plane $\boldsymbol{\alpha}_o$, where the kth circle represents the position of $\boldsymbol{\alpha}_o[k]$ by the kth closed path and the kth arrow represent the angle of $\psi[k]$ by the kth closed path. Figure 12 shows the shifts on the plane (x, y), i.e. $(\|\boldsymbol{\Delta\alpha}'_o\|, \Delta\psi)$. In Fig. 12, the kth circle represents the position $(\|\boldsymbol{\Delta\alpha}'_o[k]\|, \Delta\psi[k])$ by the kth closed path and the areas shaped as the lunes are the reachable areas Ω. Figure 13 shows the trajectory of $\boldsymbol{\alpha}_f$, where the closed paths are generated with time interval 2[sec] and the heavy lines show the values of the

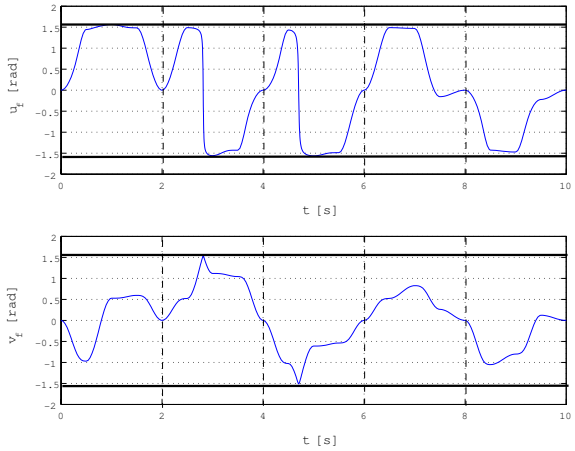

Fig. 13. Trajectory of $\boldsymbol{\alpha}_f$.

boundaries of the rolling motion θ_r. In Fig. 11, $\boldsymbol{\alpha}_o$ and ψ have converged on the target point simultaneously by five number of the iterations. Furthermore, there exist the circles $\circ$ on the dashed line from the initial point to the target point. This corresponds to the fact that the direction of the shift of $\boldsymbol{\alpha}_o$ is determined by φ such that (16) (See Fig. 4). In Fig. 12, the points of $k = 1, 2, 3$ to which the control variable shifts are the end points of the reachable areas Ω at each iteration. Next, those of $k = 4, 5$ are adjusted such that the control variable converges to the target point. These transitions show the effectiveness of the algorithm. In Fig. 13, it is evident for u_f and v_f of $\boldsymbol{\alpha}_f = [\ u_f \quad v_f\ ]^{\mathrm{T}}$ to involve in the range between $-\theta_r$ and θ_r, where $\theta_r \approx 1.56$.

VII. Conclusion

In this paper, we discussed control of contact coordinates for a contact point between a sphere and a plane with pure rolling contact by using iterative trapezoidal closed paths on the sphere with contstrained rolling motion. We first analyzed the boundary of the reachable area by the closed path with constrained rolling motion. Utilizing the result, we second proposed the method which converged all the contact coordinates to a target point by the iteration of a finite number of the closed paths. The numerical example where the rolling motion was restricted to the area on the semisphere showed the effectiveness of the proposed method.

References

[1] A. Nakashima, K. Nagase and Y. Hayakawa, "SIMULTANEOUS CONTROL OF GRASP/MANIPULATION AND CONTACT POINTS WITH ROLLING CONTACT," *Proc. 16th IFAC World Congress*, Praha, Czech Republic, 2005.

[2] D. J. Montana, "The Kinematics of Contact and Grasp," *Int. J. Robot. Res.*, Vol. 7, No. 3, pp.17–32, 1988.

[3] Z. Li and J. Canny, "Motion of two rigid bodies with rolling constraint," *IEEE Trans. Robot. Automat.*, Vol. 6, No. 1, pp. 62–72, Feb. 1990.

[4] A. Bicchi and A. Marigo, "Dexterous Grippers: Putting the nonholonomy to Work for Fine Manipulation, *Int. J. Robot. Res.*, Vol. 21, No. 5–6, pp. 427–442, 2002.